"bico-TEC" - Horizontal Conveyor Belts
Traveling in a Curved Direction

Franz KESSLER and Kari GRABNER, Austria

1. Introduction

Concerning the conveyance of bulk materials, transported volumes and haulage distances have increased over the last few decades. Of great importance are belt conveyors which satisfy not only these demands but, moreover, are adaptable as far as matching local terrain by virtue of their ability to negotiate curves.

The essential advantages of belt conveyors with horizontal curves are:

- reduction in investment costs as a result of:
  - adaptation of the belt alignment to the terrain without large civil engineering works
  - circumnavigation of barriers such as buildings, roads, streams, etc.
  - abolition of discharge and driving stations along the conveyor track
- reduction in operating costs, especially a saving in personnel costs, and a decrease in down-time in particular as a result of the elimination of discharge stations
- decrease in environmental pollution by abolition of discharge and driving stations along the conveyor track

Belt conveyors with horizontal curves are characterized by:

- incidence of a force component of the belt tensile-force in the direction of the inside curve
- unequal tensile stressing of the conveyor belt edges by running through a horizontal curve

Counteracting the force component F_T in the direction of the inside curve, which results from the belt tensile-force, while running through a horizontal curve, dead-weight forces of belt and material F_H as well as friction forces between belt and tilted idlers F_R are used, which act in the direction of the outside curve.

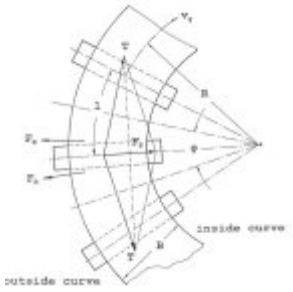

Fig.1. Forces on the conveyor belt traveling through a horizontal curve

Fig. 1 shows the forces at a section of the belt within the range of a horizontal curve. The calculation of these belt guidance-forces on conventional belt conveyors with horizontal curves is known from [1][2][3][4][8][9].

2. The new type of belt conveyor with horizontal curves

The conventional method of belt guidance was improved by a new type of horizontal curve-going belt conveyor developed by the Binder+CO AG Company Gleisdorf/Austria and the Institute of Conveying Technology and Design Methods of the Mining University of Leoben/Austria with the trade mark "bico-TEC".

With swinging idler stations, the elevation angle at the inside curve, which is necessary for the belt guidance, is self adjusting depending on the belt tensile-force and the force components of the dead weight of belt, material and swinging idler station. An exact positioning, and therefore, time-consuming installation of the idler stations before start up is not necessary.

In Fig.2 the fundamental construction of the frames for the carry-side and return-side idler-stations is shown schematically.

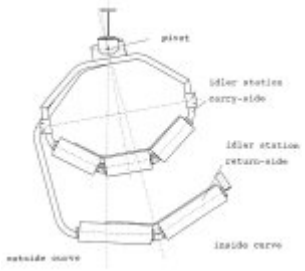

Fig.2. Carry-side and return-side idler support frames of the belt conveyor

The frames for the idler stations are freely swinging, suspended from a supporting frame.

With freely swinging idler-frames, minimum curve radii of 250 m can be achieved. Besides that, the belt is self centering for changes in the belt tensile-force.

As a result of the swinging suspension of the idler stations, deflection towards the inside of the curve forces occur, which counteract the component of the belt tensile-force.

By so doing, the gravity forces and friction forces created are in equilibrium with the component of the belt tensile-force [1][2][3][4][8][9].

With the system of "bico-TEC", changes in the belt tensile-force result not only in a lateral belt-drift but also produce a change in the suspension position.

The new type of "bico-TEC" with swinging suspended idler-stations offers three essential advantages in relation to conventional belt-conveyors with horizontal curves.

- The self adjusting support-position produces an optimum value of the horizontal guidance-force, and enables narrower curve radii than with conventional installations.
- In the case of swinging suspended idler-stations a trouble free operation of the installation is feasible, also at different extreme conditions such as changes in friction conditions or also limited movements of the soil. With conventional installations with horizontal curves, a large portion of the belt guidance is applied by frictional forces between belt and tilted idlers. Therefore these installations show a very sensitive reaction, depending on the changes of the frictional coefficient between belt and idlers. Pollution, glaciation and moisture make the frictional coefficient fluctuate within a high range, whereby the guidance forces of the belt change within large limits.
- The erection of the installation is very simple, because of the freely swinging idler frames. The exact positioning of the idlers is not necessary whereby the amount of installation work is considerably reduced.

3. Theoretical principles

The theoretical principles according to [1] to [11] are adapted to meet the new geometrical conditions of the "bico-TEC" system.
Fig.3 shows the forces, lengths and angles of the carry-side and the return-side of the belt conveyor.

The actual position of the idler frames or the value of the elevation angle is dependant on the belt tensile-force, the force components of the dead weight of the belt and bulk material, the reaction force of the belt guidance-forces from the friction between belt and tilted idlers, the lateral movement of the belt and material, as well as on the idler-frame geometry and the idler-frame weight.

At each self-adjusting idler-frame position the condition of equilibrium (1) is satisfied.

$$F_H \cdot Y - F_T \cdot Y - F_R \cdot Y + F_{geh} \cdot X = 0 \quad (1)$$

F_H is the horizontal guidance-force resulting from the components of the dead weight of belt and material, and acts in the direction of the outer curve. F_T is the force component of the belt tensile-force in the direction of the inner curve, F_R the friction force between belt and idlers, F_{geh} the force of dead weight of the idler frame and y and x are the corresponding distances of the forces to the center of the pivot point of the suspension. The indices o and u refer to the carry-side and to the return-side idler stations.

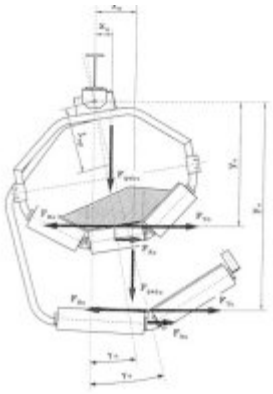

Fig.3. Forces, lengths and angles of the carry-side and return-side of the belt conveyor

3.1. Calculation of the horizontal guidance force F_H from the dead weight of belt and material

The horizontal guidance-force F_H consists of the components of the dead weight of belt and material above the individual idlers.
In Fig.4 the forces resulting from the dead weight of the belt are shown together with lengths and angles.

With the simplified assumption according to [1] the belt corresponding to its trough is divided into three longitudinal strips. The effective horizontal-force F_{HB} from the dead weight of the belt results from the sum of F_{HB} over the individual idlers. Experimental tests according to [2], have shown that the forces in the belt, parallel to the lateral idlers, are almost completely returned to the horizontal direction. As effective horizontal-force F_{HB} can therefore be represented by (2).

$$F_{HB} = F_{SB1} + F_{SBm} + F_{SB2} \quad (2)$$

The force components result from the following equations.

$$F_{SB1} = G_{B1} \cdot \sin(\lambda+\gamma) = \frac{G_B \cdot 1_T}{B} \cdot S_{B1} \cdot \sin(\lambda+\gamma) \qquad (3)$$

$$F_{SBm} = G_{Bm} \cdot \sin\gamma = \frac{G_B \cdot 1_T}{B} \cdot 1_m \cdot \sin\gamma \qquad (4)$$

$$F_{SB2} = - G_{B2} \cdot \sin(\lambda-\gamma) = \frac{- G_B \cdot 1_T}{B} \cdot S_{B2} \cdot \sin(\lambda+\gamma) \qquad (5)$$

In these equations G_B, is the meter-weight of the belt, B is the belt width, G_{Bi} are the dead-weight forces of the belt above the individual idlers, S_{Bl} and S_{B2} the supporting lengths of the belt at the lateral idlers, l_T is the distance between the idler stations, l_m the length of the central idler, λ the trough angle and γ the elevation angle of the idler station at the inside curve.

The supporting lengths of the belt at the lateral idlers result from Fig.5.

$$S_{B1} = S_0 + S_B \qquad (6)$$

$$S_{B2} = S_0 - S_B \qquad (7)$$

The length S_0 is the supporting length of the belt at the lateral idlers with central belt-position and S_B the lateral drift of the belt.

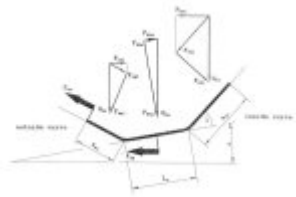

Fig.4. Forces, lengths and angles in the belt trough with an unloaded belt

Fig.5. Lengths with lateral belt-drift

Similar relationships can be considered for horizontal guidance-forces resulting from the bulk-material loading. Forces, areas, lengths and angles are shown in Fig.6.
Corresponding to equation (2) the horizontal force F_{HG} can be presented by (8) with

$$F_{HG} = F_{SG1} + F_{SGm} + F_{SG2} \qquad (8)$$

$$F_{SG1} = G_{G1} \cdot \sin(\lambda + \gamma) \qquad (9)$$

$$F_{SGm} = G_{Gm} \cdot \sin\gamma \qquad (10)$$

$$F_{SG2} = - G_{G2} \cdot \sin(\lambda - \gamma) \qquad (11)$$

G_{Gi} are the forces of the dead weight of the bulk-material loadings above the individual idlers and are calculated from the equations (12) to (14).

$$G_{G1} = A_{X1} \cdot 1_T \cdot e \qquad (12)$$

$$G_{Gm} = A_{Xm} \cdot 1_T \cdot e \qquad (13)$$

$$G_{G2} = A_{X2} \cdot 1_T \cdot e \qquad (14)$$

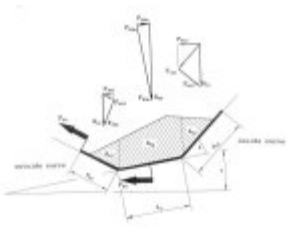

Fig.6. Forces, lengths and angles in the belt trough with a loaded belt

A_{xi} are the cross sections of bulk material above corresponding idlers with laterally-drifted belt, l_T is the distance between idler stations and ρ the bulk density.

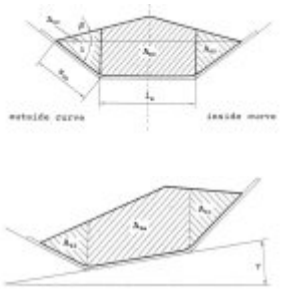

Fig.7. Details of bulk material cross-sections at central position of belt and bulk material according to DIN 22101 (above). Lateral elevation and lateral drift of belt and material (below)

For the calculation of the momentary cross-sections of bulk material with lateral belt-drift one starts with the cross sections at the central position of the belt and the material.

Fig.7 shows the cross section at the central position with lengths and angles.

$$A_{S0} = ½ \cdot S^2_{0G} \cdot \cos\lambda \cdot (\sin\lambda + \cos\lambda \cdot \tan\beta) \qquad (15)$$

$$A_{M0} = 1_m \cdot (S_{0G} \cdot \sin\lambda + S_{0G} \cdot \cos\lambda \cdot \tan\beta + 1_m \cdot \tan\beta/4) \qquad (16)$$

A_{S0} is the initial cross-section of the bulk material at central belt and material position according to DIN 22101 above the lateral idler, A_{M0} is the corresponding area above the central idler. λ is the trough angle and ß the dynamic discharge-angle of the bulk material. S_{0G} is the supporting length of the material at the lateral idler at central position of the belt and material.

The cross sections of material A_{Xl}, A_{X2} and A_{Xm} at lateral drift of belt and material, result from the equations (17) to (19) according to [2][5].

$$A_{X1} = A_{S0} \cdot \left(1 + \frac{\xi_1 \cdot S_B}{S_0}\right)^{1,7} \qquad (17)$$

$$A_{XM} \approx A_{M0} \qquad (18)$$

$$A_{X2} = A_{S0} \cdot \left(1 - \frac{\xi_2 \cdot S_B}{S_0}\right)^{1,7} \qquad (18)$$

The factors ξ1 and ξ2 indicate to what extent the bulk material follows the lateral belt-drift, in the direction of the inside curve. At the inside of the curve most of the bulk materials follow the belt to 75%, that means ξ=0,75, at the outside curve generally to 50% that means ξ2=0,5. [2][5]

The total horizontal guidance-force F_H is arrived at by addition of the individual components of the dead weight of the belt and material.

$$F_H = \Sigma F_S = F_{SB1} + F_{SBm} + F_{SB2} + F_{SG1} + F_{SGm} + F_{SG2} \qquad (20)$$

With $G_i=G_{Bi}+G_{Gi}$ and the equations (3) to (5) and (9) to (11) we get

$$F_H = G_1 \cdot \sin(\lambda + \gamma) + G_m \cdot \sin\gamma - G_2 \cdot \sin(\lambda-\gamma) \qquad (21)$$

3.2. Calculation of the frictional forces between belt and tilted idlers

The frictional forces are dependant on the normal forces affecting the idlers and on the friction coefficient between belt and tilted idlers. Fig.8 shows the frictional forces at the idlers of an idler station V_g is the direction of the belt and ψ_i are the tilt angles of the individual idlers.

The normal forces from the dead weight of the belt above the idlers result from the equations (22) to (24) according to [1][2][7][10][11].

$$F_{NB1} = G_{B1} \cdot \cos(\lambda + \gamma) \qquad (22)$$

$$F_{NBm} = G_{Bm} \cdot \cos\gamma \qquad (23)$$

$$F_{NB2} = G_{B2} \cdot \cos(\lambda - \gamma) \qquad (24)$$

The values of normal forces on the individual idlers are also influenced by the troughability of the belt [2][3][4][6].

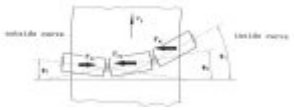

Fig.8. Top view of the trough showing the idler-tilt positions

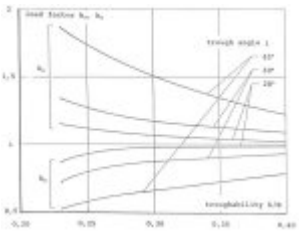

Fig.9. Load factors k_s and k_M of the lateral and central idler depending on the troughability h/B according to ISO 703 and the trough angle λ

To consider the troughability, the normal forces at the lateral idlers are to be multiplied with the load factor k_s>1, and the normal forces at the central idler with the load factor k_M < I according to Fig.9.
Depending on the troughability of the belt the effective normal-forces increase slightly at the lateral idlers and decrease insignificant at the central idler.

The normal forces of the dead weight of the material result from the equations (25) to (27)

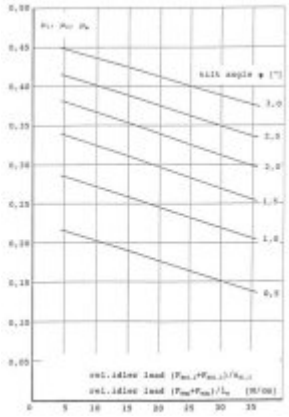

Fig. 10. Frictional coefficients μ_1, μ_2 and μ_m depending on the relational load on the idlers and the tilt angle

$$F_{NG1} = G_{G1} \cdot \cos(\lambda + \gamma) \qquad (25)$$

$$F_{NGm} = G_{Gm} \cdot \cos\gamma \qquad (26)$$

$$F_{NG2} = G_{G2} \cdot \cos(\lambda - \gamma) \qquad (27)$$

The corresponding normal-forces from the dead weight of the belt and the bulk material are to be added. By multiplying the normal forces with the friction coefficient μ according to Fig. 10, we get the friction forces of the individual idlers. [1][3]

$$F_{Ri} = F_{Ni} \cdot \mu_i \qquad (28)$$

The total guidance-force of the belt resulting from the friction between belt and tilted idlers is obtained by addition of the individual friction-forces F_{R1}, F_{Rm} and F_{R2}.

$$F_R = F_{R1} + F_{Rm} + F_{R2} \qquad (29)$$

3.3 Calculation of the elevation angle γ

The formulae according to chapter 3.1. and 3.2. are set into the equation of the equilibrium (1) for the idler frame. After transforming this equation the elevation angle γ can be shown explicitly. By so doing, for simplification, cosγ=l is used in the equation since elevation angle γ generally has only small values.

$$\gamma = \arcsin \frac{\dfrac{F.1_T}{R}}{\dfrac{F_{geh}.1_{sp}}{y}} \cdot \frac{+ G_1.(\mu_1.\cos\lambda - \sin\gamma) + G_m.\mu_m + G_2.(\sin\lambda - \mu_2.\cos\lambda)}{+G_1.(\cos\lambda + \mu_1.\sin\lambda) + G_m + G_2.(\cos\lambda + \mu_2.\sin\lambda)} \qquad (30)$$

F is the belt tensile force, R the radius of a horizontal curve and F_{geh} the dead weight of the idler frame. l_{sp} is the distance between the center of gravity and the pivot of the idler frame according to Fig.3. By approximate analysis of the frictional coefficients μ_1, μ_m and μ_2 according to Fig. 10 the equation is solvable. First of all a permissible lateral belt-drift S_B is chosen. With the equations (3) to (5), (6), (7) and (12) to (14) values for G_1, G_m and G_2 are established and the elevation angle γ is determined.

Next, a check is carried out, using the calculated elevation-angle γ, whether the additional conditions for equilibrium according to equation (31), which are important for belt guidance, are met.

$$F_H + F_R = F_T \qquad (31)$$

The belt guidance in the idler trough is guaranteed if F_H+F_R is bigger than F_T. But in this case the actual adjusting-angle is smaller than the calculated angle γ. In the calculation of the belt conveyor the actual adjusting elevation-angle at the carry and return-side is of great interest because it must be checked that the carry-side belt is not running into the idler frame of the return-side belt.
The angle results from achieving the condition of equilibrium (31) and is established iteratively by varying the lateral belt drift S_B
The calculation is carried out for the unloaded and loaded belt at the idler station, in the section of the horizontal curve where the belt tension-force is greatest. The minimum possible radii of the horizontal curves are shown in Fig. 11 depending on the belt tensile-force and the belt width.

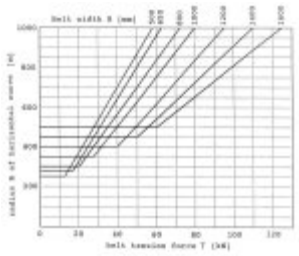

Fig.11. Radius R of the horizontal curve depending on the belt tensile-force T and the belt width B

The diagram is valid for loaded and unloaded EP-belts, three idlers with the same length in the carry-side and two idlers in the return-side according to DIN 22107, a trough angle of 40° in the carry-side and 17° in the return-side. The tilt angle of the lateral idlers is 0,5°, the skewed position of the total idler-station in the direction of the outside curve is 0,5°. When establishing the diagram, the additional elongation of the belt edges was kept constant with ε_{add}=0,15%. By so doing the horizontal lines to the left of the diagram can be explained.
The radii shown in Fig. 11 are in each case the largest minimum radii resulting from the calculation of the loaded and unloaded belt. As belt loading, the cross-sectional areas according to DIN 22101 were assumed.
In the figure only belt widths up to 1600 mm are shown. Larger belt widths are also possible.

4. Example of an installed "bico-TEC" - belt conveyor

Since 1986 several belt conveyors of this type were installed in Europe and in Far East. Fig. 12 shows the alignment of the horizontal curve of two parallel belt conveyors in Papua New Guinea, which run through a radius of 350 m.

Fig.12. Alignment of the horizontal curve of the belt conveyors

The first conveyor transports ore from the mine to the preparation plant, and the second conveyor returns the waste as backfill to the underground.
Fig.13 shows the belt travel of the unloaded carry-side and Fig.14 shows the belt travel of the loaded carry-side of a belt conveyor in Germany.

Fig. 13. Belt travel of the unloaded carry-side

Fig.14. Belt travel of the loaded carry-side

The idler frame is a pipe construction. The supporting frame, within which the swinging idler-frame is suspended is constructed out of pipe and sectional steel. Fig. 15 shows the idler frames of the return-side.

Fig.15. Idler frames of the return-side

5. Summary

Proceeding from the basic calculations for conventional belt-conveyors with horizontal curves a new type of horizontal curve going belt-conveyor with the trade mark "bico-TEC" was developed in co-operation between the BINDER+CO AG Company, Gleisdorf/Austria and the Institute of Conveying Technology and Design Methods of the Mining-University of Leoben.
An essential characteristic of the new type "bico-TEC" are the swinging suspended idler-stations in carry-side and return-side, which are self adjusting to achieve the optimal position for belt guidance. This adjustment occurs as a result of the dependence on the belt tensile-force, the components of the dead weight of belt, bulk material and idler frame as well as on the frictional forces between belt and tilted idlers. By the adaption of the idler-frame position, to the momentary conditions, narrower curve radii are possible compared to conventional belt-conveyors with horizontal curves.

6. References

1. GRIMMER, K.-J. and BEUMER, B.
   Auslegung und Betrieb kurvengängiger Förderbänder mit normalen Fördergurten. Fördern und Heben 22 (1972), No.3, pp.107-112 and No.4, pp.174-178
2. KESSLER, F.
   Untersuchung der Führungskräfte quer zur Gurtlaufrichtung bei Gurtförderern mit Horizon-talkurven. Dissertation 1986, Montanuniversität Leoben
3. GRIMMER, K.-J. and KESSLER, F.
   Spezielle Betrachtungen zur Gurtführung bei Gurtförderern mit

Horizontaikurven. Teil I: Anmerkungen zum herkömmlichen Berechnungsverfahren. Berg- und Hüttenmännische Monatshefte, 132 (1987), No.2, pp.27-32
4. GRIMMER, K.-J. and KESSLER, F.
Spezielle Betrachtungen zur Gurtführung bei Gurtförderern mit Horizontaikurven. Teil II: Verbesserung des herkömmlichen Berechnungsverfahrens. Berg- und Hüttenmännische Monatshefte, 132 (1987), No.6, pp.206-211
5. KESSLER, F.
Untersuchungen des Schüttgutverhaltens bei seitlicher Auswanderung des Gurtes in der Tragrollenmulde einer Gurtförderanlage. Berg-und Hüttenmännische Monatshefte, 134 (1989), No.2, pp.35-40
6. KESSLER, F.
Einfluß der Muldungsfähigkeit des Fördergurtes auf die Verteilung der Normaikräfte zwischen Gurt und Tragrollen.
Hebezeuge und Fördermittel, 30 (1990) No.1, pp.8-11
7. GRABNER, K.
Untersuchungen zum Normalkraftverlauf zwischen Gurt und Tragrollen bei Gurtförderern. Dissertation 1990, Montanuniversität Leoben
8. GRIMMER, K.-J. and KESSLER, F.
Zur Auslegung von Gurtförderern mit Horizontalkurven. Fördern und Heben, Vereinigte Fachverlage Krausskopf 41 (1991), No.5, pp.428-432
9. GRIMMER, K.-J. and KESSLER, F.
The Design of Belt Conveyors with Horizontal Curves. Bulk Solids Handling, 12 (1992), No.4, pp.557-563
10. GRIMMER, K.-J. und GRABNER K.
Untersuchungen über die Normalkräfte zwischen Gurt und Tragrollen an kritischen Stellen des Gurtverlaufes bei Bandförderanlagen. Berg-und Hüttenmännische Monatshefte, 138 (1993), Nr.6, pp.212-220
11. GRABNER, K., GRIMMER, K.-J. and KESSLER, F.
Investigation into normal forces between belt and idlers at critical locations on the belt-conveyor track. Bulk Solids Handling, 13 (1993), No.4, pp. 727-734